J. Braz. Chem. Soc., Vol. 8, No. 6, 581-586, 1997.
Printed in Brazil.

0103 – 5053 $6.00 + 0.00

Article

Characterization of a Brazilian Smectite by Solid State NMR and X-Ray Diffraction Techniques

Alcides Wagner Serpa Guarino[a], Rosane A. S. San Gil[a*], Helena Polivanov[b], and Sonia M.C. Menezes[c]

[a]CCBS/Uni-Rio and Instituto de Química, Univ. Federal do Rio de Janeiro, CT, bloco A/605, Ilha do Fundão, 21949-900 Rio de Janeiro, Brazil

[b]Departamento de Geologia, Instituto de Geociências da UFRJ

[c]Divisão de Química, Centro de Pesquisas da Petrobras

Received: July 9, 1997

As técnicas de difração de raios-X (DRX), análise térmica diferencial (ATD) e ressonância magnética nuclear no estado sólido com rotação no ângulo mágico (RMN-MAS) de ^{27}Al e ^{29}Si foram utilizadas para o monitoramento das etapas de fracionamento de uma amostra de esmectita brasileira, previamente moída, originária de Campina Grande, Paraíba, e utilizada como matéria-prima para a preparação de catalisadores ácidos. As frações foram obtidas por tratamentos físico e químico. As análises de DRX das frações areia e silte mostraram que ambas possuem predominantemente quartzo e feldspato, respectivamente. Os resultados de DRX da fração argila, saturada com K^+ e aquecida, confirmaram tratar-se de argilomineral do grupo 2:1, enquanto a análise da fração argila, saturada com Mg^{2+} e glicolada, confirmou a presença de esmectita. Os resultados de RMN-MAS de ^{27}Al e ^{29}Si evidenciaram ser a fração areia constituída por cerca de 79% de quartzo; a fração silte possui 55% de quartzo, e a fração argila, rica em esmectita com baixa substituição isomórfica de Si por Al, contém 38% de quartzo.

X-ray diffraction (XRD), differential thermal analysis (DTA) and ^{27}Al and ^{29}Si solid state MAS-NMR techniques were used to monitor the fractionation steps of a brazilian smectite, previously crushed, from Campina Grande, Paraíba. The sand, silt and clay fractions were obtained by physical and chemical treatments. The XRD analysis of sand and silt fractions showed that both fractions had predominant quartz and feldspar, respectively. The XRD results of the K^+ saturated and heated clay fraction confirmed that the natural clay belongs to the 2:1 clay-mineral group, whereas the analysis of the Mg^{2+} saturated and glycolated clay fraction confirmed the presence of a smectite group clay. The MAS-NMR results of ^{27}Al and ^{29}Si showed that the sand fraction contains 79% of quartz and the silt fraction contains 55% of quartz, while the clay fraction is rich in smectite with low isomorphic replacement of Si by Al, and contains 38 % of quartz.

Keywords: *smectite, solid-state NMR, X-ray diffraction*

Introduction

Natural clays were among the earliest solid acid catalysts used in the oil industry to promote cracking and isomerization reactions. The development of new catalysts with high activity and good thermal stability has lead to the study of new materials from natural clays[1]. Owing to growing environmental concerns over the disposal of depleted acid catalysts, there is interest in replacing traditional catalysts, such as aluminum chloride and hydrofluoric acid, by recyclable solid acids. Since the early 1950's many attempts have been made to develop artificial methods of introducing interlayers into expandable silicates[2]. In the midst of natural clays, smectites are important as the interlayer ions distance can be modified, by changing the ions interlayer with other cations and complexes, which allows

The results of this paper were presented at the 5th Brazilian NMR Meeting, Angra dos Reis, Brazil, May 1995, and at the 18th Annual Meeting of the Brazilian Chemical Society, Caxambú, Brazil, June 1995.

the end-product to acquire advantageous chemical properties. Smectite is often a dominant clay in soils formed under alkaline weathering conditions[3].

Natural clays contain varying percentages of clay-grade materials: non-clay and clay mineral components. In general, fine-grained materials (< 2 μm)[4] have been called clay so long as they had distinct plasticity and small amounts of coarse material, to warrant the appellations silt (2-50 μm) and sand (> 50 μm)[5].

High resolution solid-state NMR spectroscopy is recognised as an important and sometimes indispensable complementary technique to traditional diffraction methods[6]. NMR is sensitive to short-range ordering, local geometries, and local symmetry, whereas X-ray diffraction studies average much longer range periodicities and ordering. ^{29}Si and ^{27}Al solid state NMR experiments are of fundamental interest because they can provide complementary structural information to that determined by diffraction techniques.

Magic Angle Spinning (MAS) is one of the line-narrowing techniques available, which significantly improves the resolution of peaks in the NMR spectrum of a solid, and allows direct determination of the isotropic chemical shift. ^{29}Si and ^{27}Al MAS NMR have been extensively used to analyse aluminosilicates such as clays. Since silicon has a low chemical shift anisotropy (CSA), the line broadening can be removed at easily achievable spinning rates, whereas ^{27}Al requires high field and high spinning rates to overcome the quadrupolar interactions[7]. Of particular relevance and importance is the direct determination of the amount of non-clay material present in the Brazilian clay and the isomorphic substitution of Si by Al at the tetrahedral sites of the aluminosilicates.

The aim of this work was to use X-ray diffraction (XRD), differential thermal analysis (DTA) and solid state nuclear magnetic resonance of ^{29}Si and ^{27}Al (MAS-NMR) techniques to monitor the fractionation steps of a raw material from Campina Grande, Brazil. The NMR data (*e.g.*, number of peaks, individual peak intensities and chemical shifts) were used to characterise the different fractions obtained.

Experimental

Fractionation of the raw material

The previously crushed raw material (sample 1) from Campina Grande (PB, Brazil) was passed through a 270 mesh sieve. There are several types of soil treatment mentioned in literature[3,8,9,10], used to characterise the samples by X-ray analysis. We followed the procedure suggested by Math[3]. The sand fraction (sample 2) was separated by sieving. The silt (sample 3) and clay (sample 4) fractions were separated by decantation. The clay fraction was subjected to a treatment which involved dissolution of soluble salts and carbonates with sodium acetate buffered at pH 5, followed by oxidation of organic matter with 30 per cent hydrogen peroxide. Iron oxides were removed by sodium dithionite-citrate-bicarbonate treatment[4] (sample 5). This fraction was then saturated with Mg^{2+} (sample 6) and K^+ (sample 7); The sample 6 was glycolated and the sample 7 was heated to 823 K for 1 h before XRD analysis[4].

Characterization and measurements

XRD analysis of oriented fractions were made using a Rigaku-Geigerflex 2013 diffractometer equipped with a proportional counter and pulse height analyser using Ni filtered CuKα radiation, produced under conditions of 40 kV and 30 mA. Diffraction patterns were collected at a scanning rate of 4^o (2θ)/min in the interval of 2° and 70°.

Thermal analysis (DTA) was performed using a Rigaku-TG termoflex 8110-TAS100 thermal analyser. The chemical analysis was determined by atomic absorption spectrophotometry[11], using a VARIAN AA6 spectrophotometer.

The cation exchange capacity (CEC) was determined by flame emission spectrophotometry[12] as 74 meq/ 100 g clay: 1 g of material (natural clay) was weighed and exchanged (through centrifugation) with a K^+ solution. The suspension was washed with ethanol 95%, and the aqueous phase was discarded. Then, the K^+ was exchanged by NH_4^+ ion five times and the resulting solutions were collected in a volumetric flask. The amount of K^+ ion in this solution was determined by flame spectrometry, using a flame photometer MICRONAL B262.

The chemical analysis of the raw material[11] was: SiO_2, 61.60%; Al_2O_3, 15.30%; Fe_2O_3, 6.40%; MgO, 2.60%; Na_2O, 1.40%; TiO_2, 1.10 %; CaO, 1.00% K_2O, 0.54%; H_2O, 10.05%; the P, Cr, Zn, Mn and Sr elements were present in less than 300 ppm.

Solid state NMR measurements were carried out on a Varian VXR-300 spectrometer operating at a B_0 of 7.05 Tesla (corresponding to a Larmor frequency of 59.6 MHz for silicon and 78.2 Mhz for aluminum). A single pulse sequence was used with quadrature detection for both nuclei. The magic angle was accurately adjusted prior to data acquisition using KBr. Samples were spun in zirconia rotors equipped with Kel-F caps, at speeds of 3 kHz for ^{29}Si, and 7 kHz for ^{27}Al. A 2.5 μs (30°) pulse was used for silicon, with pulse delay of 120 s, for quantitative analysis[13]. For aluminum experiments a short pulse of 0.7 μs ($\pi/12$) was chosen, so that the results could be quantitatively exploited (flip angle $\pi/2l+1$). The recycle time was 0.2 s. About 5000 and 500 scans were needed to obtain ^{27}Al and ^{29}Si spectra of the samples. The ^{29}Si signal positions were referenced using a secondary standard of caulim (δ = -91.5 ppm), in relation to TMS, while the ^{27}Al chemical shifts were referenced using a solid sample of $AlCl_3.6H_2O$ (δ = 0 ppm).

Results and Discussion

DTA analysis

The differential thermal analysis (DTA) of the raw material (Fig. 1) showed an intense endothermic peak at 110 °C. This peak could be due to water molecules adsorbed in the interlayer or coordinated with exchangeable cations. The form and position of this peak depend on the nature of the adsorbed cation and on the smectite clay mineral. In this case, these cations are probably Na^+ and K^+. The peak observed at 550 °C is a characteristic one, and would be due to loss of structural hydroxyls in iron rich smectites. Santos[14] pointed out that the crystalline structure of the smectite is preserved after the loss of the hydroxyl groups until 800 °C. Above 800 °C, a double peak, endo-exothermic, appeared at 890 °C and 920 °C, respectively. The endothermic peak represents the destruction of the crystalline framework, while the exothermic peak represents the formation of α or β mulite quartz.

XRD analysis

Figure 2 shows the XRD patterns of the samples 1 to 7. Table 1 shows the reflections for the oriented samples (a diffractometer pattern from a strongly oriented clay specimen may show only the 00*l* series of basal reflections with small or no evidence of hk*l* reflections)[15].

The sample 1 showed a peak at 14.9 Å (2θ = 5.9°). The Mg^{2+} and K^+ saturations, following treatment with ethylene glycol and heating at 823 K, respectively, confirmed the presence of a clay mineral of the smectite group, through the 001 peak for 17.0 Å (2θ = 5.2°) (sample 6, Fig. 2) and breakdown to 10.0 Å (2θ = 8.8°) (sample 7, Fig. 2)[4]. The peaks at 4.26 Å (2θ = 20.9°); 3.33 Å (2θ = 26.7°) and 3.25 Å (2θ = 27.4°) suggest the presence of quartz and feldspar, respectively, in the raw material.

The sample 2 showed a strong reflection corresponding to 3.33 Å and a minor one at 3.25 Å, suggesting that quartz was a predominant mineral in this fraction. Quartz was also a predominant mineral in sample 3, as a strong peak appeared at 3.33 Å. This sample also showed a peak at 14.9 Å which indicated the presence of smectite. This could be justified as a result of pre-crushing of the original material and the difficulty to separate the fractions by decantation. The clay mineral corresponding peak of a smectite group in sample 5 was more pronounced than in sample 4, due to the CBD treatment.

The precision of the peak intensities for values below 2θ = 5° is relatively small; the clay mineral of the smectite

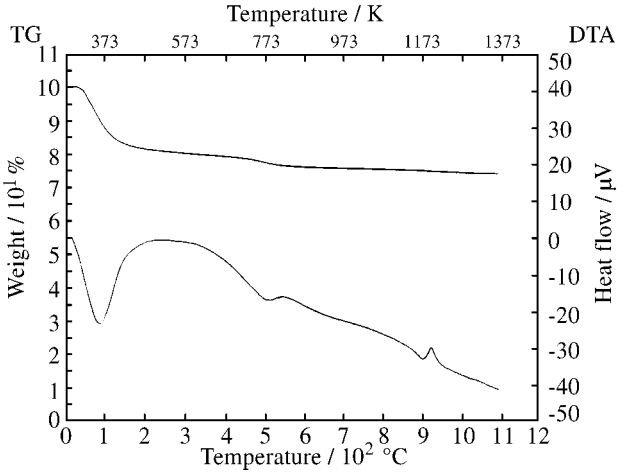

Figure 1. DTA of the raw material (sample 1).

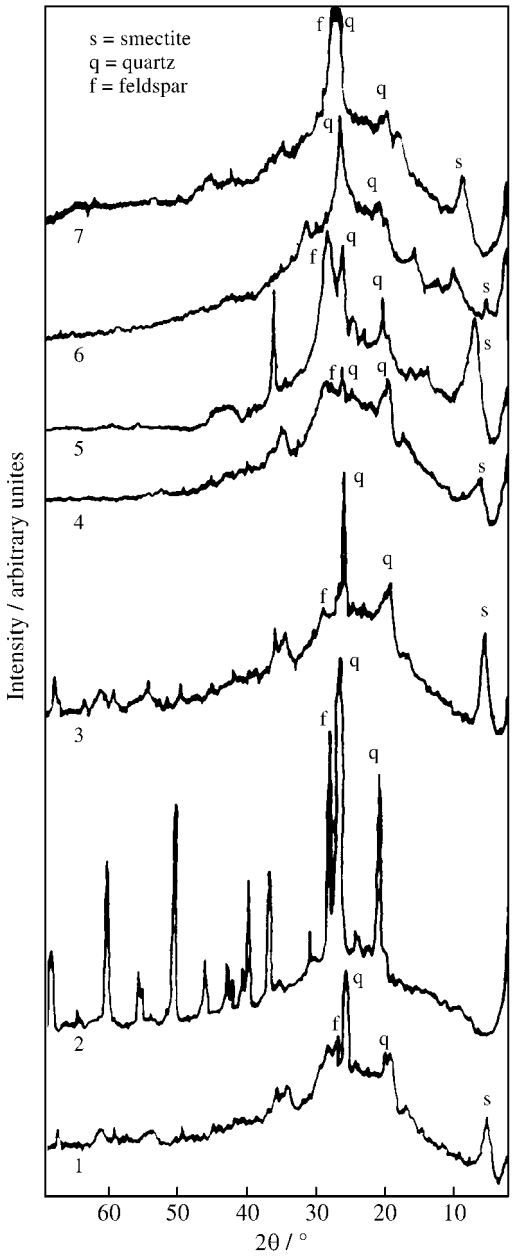

Figure 2. XRD of the fractions 1 (raw material); 2 (sand fraction); 3 (silt fraction); 4 (clay fraction); 5 (clay fraction without iron oxides); 6 (sample 5 with Mg^{2+}, glycolated) and 7 (sample 5 with K^+, heated at 823 K).

group presented in this work was identified by the increase and decrease of the 001 peak, as observed in Fig. 2, samples 6 and 7.

The sample 6 showed an expanded peak corresponding to 17.0 Å while sample 7 showed a peak at 10.0 Å, indicating that smectite is the dominant mineral 2:1. It suggests the predominance of hydroxyl interlayered smectite in the fine clay fractions[3]. These results are similar to those of Volzone[17,18], for argentine bentonite, although our sample is not a bentonite.

^{27}Al NMR spectra

For ^{27}Al, which has spin I = 5/2, the m= 1/2 → m=-1/2 transition is independent of first order quadrupolar interaction but is affected by second-order quadrupolar effects. Large variations of the quadrupole coupling constant provoked distortion of the peak shape because of the increasing influence of second-order terms. The sideband pattern is also modified. The quadrupole coupling constant being the product of the quadrupole moment by the electrical field gradient at the nucleus, the peak shape is very sensitive to a change in the symmetry of the coordination shell and in the distribution of electrical charges. Here also in first approximation, the weaker the shielding, the more sensitive the shift. The highest available field, namely 7.05 T, was used for ^{27}Al in order to decrease as much as possible the effect on the shift of the second-order quadrupolar effect[19].

The ^{27}Al MAS-NMR spectra of the samples are shown in Fig. 3. The spectra consist of one or two principal components and a series of sidebands associated to the spinning of the samples. The line around 0 ppm must be assigned to octahedral Al sites and the line at 56 ppm to tetrahedral Al ions. These assignments are in agreement with the structural compositions of the samples.

The amounts of Al^{IV} and Al^{VI} for each sample were indicated in Table 2.

In the raw material (sample 1) both Al^{IV} and Al^{VI} were present. The tetrahedral aluminum sites would be present

Table 1. XRD data of the fractions 1 (raw material); 2 (sand fraction); 3 (silt fraction); 4 (clay fraction); 5 (clay fraction without iron oxides).

Sample	2θ	d (Å)	hkl[16]	mineral
1	5.9	14.9	001	smectite
	20.8	4.26	100	quartz
	26.7	3.33	101	
	27.3	3.25	002	feldspar
2	20.8	4.26	100	quartz
	26.7	3.33	101	
	27.3	3.25	002	feldspar
3	5.9	14.9	001	smectite
	20.8	4.26	100	quartz
	26.7	3.33	101	
	27.3	3.25	002	feldspar
4	5.9	14.9	001	smectite
	20.8	4.26	100	quartz
	26.7	3.33	101	
	27.3	3.25	002	feldspar
5	7.2	12.3	001	smectite
	20.8	4.26	100	quartz
	26.7	3.33	101	
	27.3	3.25	002	feldspar

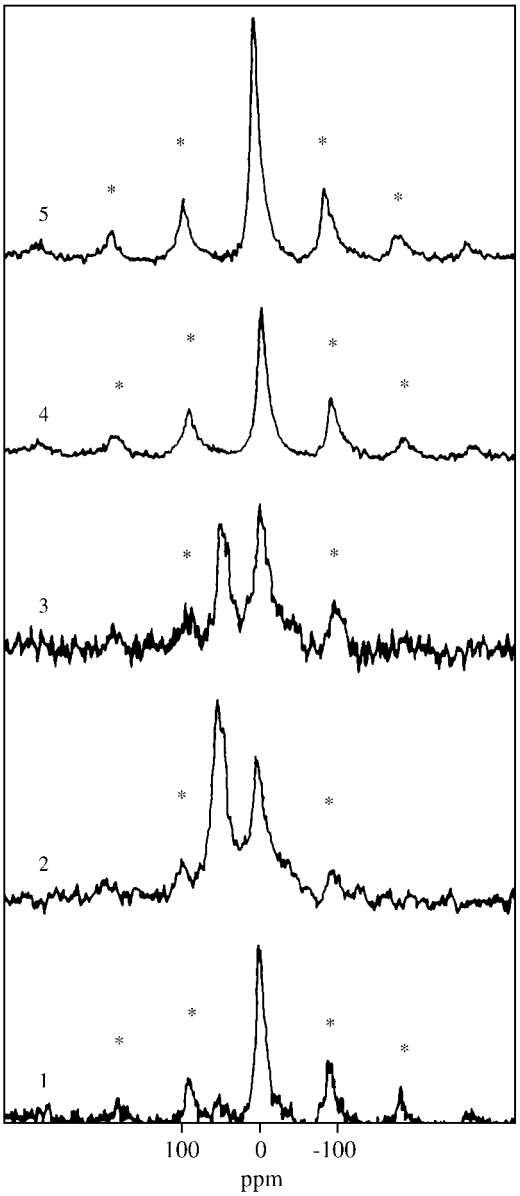

Figure 3. ^{27}Al MAS NMR spectra of the fractions 1 (raw material); 2 (sand fraction); 3 (silt fraction); 4 (clay fraction); 5 (clay fraction without iron oxides). The spinning sidebands are labelled*.

Table 2. Percentage composition of tetrahedral and octahedral aluminum and of Si^3 (nAl) and Si^4 (0Al) in the samples 1 (raw material); 2 (sand fraction); 3 (silt fraction); 4 (clay fraction); 5 (clay fraction without iron oxides) obtained by MAS-NMR of ^{27}Al and ^{29}Si.

Samples	% $Al_{TETR.}$	% $Al_{OCT.}$	% Si(nAl)	%Si(0Al)
1	7.0	93.0	57	43
2	44.2	55.8	21	79
3	31.6	68.4	45	55
4	1.5	98.5	64	36
5	0.6	99.4	62	38

both in the structure of feldspar and smectite, in the case of isomorphic substitution of silicon in the tetrahedral sheet. In samples 2 and 3 the Al^{IV} signal was more intense than in samples 1, 4 and 5, thus showing that probably it corresponds to the aluminum present in the feldspar mineral, in accordance with the DRX results for these samples. The amount of the octahedral aluminum site, only present in the smectite framework (chemical shift at 3.5 ppm), was higher in sample 5, and lower in samples 2 and 3. These results showed that the clay mineral exists in all the fractions, as a consequence of the previous crushing of the raw material.

^{29}Si NMR spectra

For the ^{29}Si nucleus (spin = 1/2) the chemical shift is affected mainly by the electronic density on the oxygen atoms of the silicon tetrahedron. Therefore the nature of the neighbouring atoms, linked or coordinated to these oxygen atoms, may influence the shift. The more positive the chemical shift, the weaker the shielding. The spread of those shifts is not only a function of the structural disorder but it depends on the nature of the second neighbours[20]. This may be the reason why for the same next nearest neighbours there are significant differences between phyllosilicates and tectosilicates.

The ^{29}Si MAS NMR spectra of the different samples are given in Fig. 4. The NMR spectra of the samples showed two components that appeared in the range -70 to -93 ppm (smectite framework) and -107.1 to -107.6 ppm (α-quartz)[6]. The composition of these samples are indicated in Table 2.

The ^{29}Si chemical shift (ppm) of the main peak is from -92.8 to -93.6 ppm, in the samples 1 to 5. It corresponds to (Q^3nAl) sites, which is consistent with data about smectites. The secondary one is around -107.4 ppm, similar to that of α-quartz[21].

The signal of α-quartz (Q^4OAl) was very high in samples 2 and 3, and lower in sample 5. The signal with a chemical shift centered at -93 ppm, increased in intensity in the order: sample 2 < sample 3 < sample 4, which confirmed the gradative enrichment in smectite with the treatment employed. These results are consistent with XRD analysis.

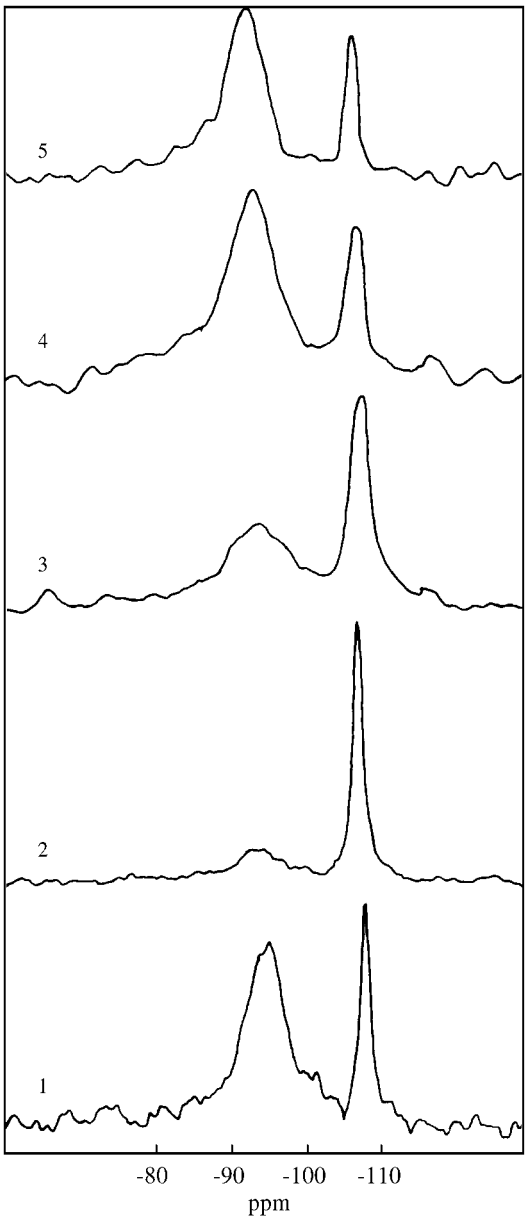

Figure 4. ^{29}Si MAS NMR spectra of the samples 1 (raw material); 2 (sand fraction); 3 (silt fraction); 4 (clay fraction); 5 (clay fraction without iron oxides).

In samples containing iron in the octahedral sheet the lines are considerably broadened by paramagnetic interactions and the fine structure of the NMR spectra is lost. The problems caused by paramagnetism in the solid state (signals enlarged and, in extreme cases, no visualisation of the signal), leads to the necessity for removal of Fe^{3+} species with sodium dithionite, in the case of soil amounts[22,23]. The citrate-bicarbonate-dithionite (CBD) extraction procedure was developed for removing pedogenic iron oxides from

clays[24], but the lithogenic iron oxides remained in the aluminosilicate framework[25].

The results obtained with ^{29}Si MAS-NMR spectra confirmed the expected increase in the relative area of (Q^3nAl) silicon sites after the chemical treatment with CBD (sample 5). The prominent sidebands still present in the ^{27}Al and ^{29}Si spectra of the treated sample could be due both to the presence of iron within the aluminosilicate lattice[26] (probably in the octahedral sheet) or the presence of iron oxides not removed by the CBD method.

Conclusions

In this work we have demonstrated that ^{29}Si MAS-NMR and ^{27}Al MAS-NMR combined with XRD and DTA is a powerful method for the study of different fractions of clay minerals. Qualitative XRD measurements were in accordance with the results of NMR, and were able to determine the distribution of the different minerals in each of the fractions. Although the ideal composition of a smectite contains only Al^{VI}, in the sample of a brazilian smectite studied there is a small amount of Al^{IV} for Si substitution in the tetrahedral sheet. The amount of quartz diminished with the fractionation although it was around 37 % in a clay-rich fraction, probably due to the fact that the raw material was crushed.

Acknowledgments

The authors thank U.B.M. do Brasil for providing the clay sample. A.W.S.G. thanks CAPES for a doctoral fellowship.

References

1. Figueras, F. *Catal.-Rev. Sci. Eng*. **1988**, *30*, 457.
2. Rich, C.I. *Clays & Clay Min.* **1968**, *16*, 15.
3. Math, S.K.N.; Murthy, A.S.P. *Appl. Clay Science* **1994**, *9*, 303.
4. Jackson, M.L. In *Soil Chemical Analysis- Advanced Course*, 2nd Ed., Published by the author, Dept. of Soil Science, Univ. of Wisconsin, U.S.A., 1974.
5. Grim, R.E. *Clay Mineralogy*, McGraw-Hill Books Co., New York, 1968.
6. Engelhardt, G.; Michel, D. In *High Resolution Solid-State NMR of Silicates and Zeolites*, John Wiley & Sons, U.S.A., 1987.
7. Asseid, F.; Miller, J.M.; Clark, J.H. *Can. J. Chem*. **1992**, *70*, 2404.
8. del Riego, A.; Herrero, I.; Pesquera, C.; Blanco, C.; Benito, I.; González, F. *Appl. Clay Sci*ence **1994**, *9*, 189.
9. Skjemstad, J.O.; Clarke, P.; Taylor, J.A.; Oades, J.M.; Newman, R.H. *Aust. J. Soil Res*. **1994**, *32*, 1215.
10. Selvaraj, S; Mohan, B.V.; Krishna, K.N.; Jai Prakash, B.S. *Appl. Clay Science* **1996**, *10*, 439
11. Leite, S.Q.M. In *Estudo da Pilarização de Argilas com Complexos de Alumínio*, MSc. dissertation, PEQ-COPPE/UFRJ.,1993.
12. Jackson, M.L. In *Soil Chemical Analysis* , Prentice-Hall of India P. Ltd., 1967, p.59.
13. Guarino, A.W.S.; Menezes, S.M.C.; Dieguez, L.C; San Gil, R.A.S. In *Book of Abstracts*, 6th Brazilian NMR Meeting, 1997, p.78.
14. Santos, P.S. In *Ciência e Tecnologia de Argilas* , Ed. Edgard Blücher Ltda., Vol. I, São Paulo, Brasil, 1992.
15. Brown, G.; Brindley, G.W. In *Crystal Structures of Clay Minerals and their X-ray Identification*; Edited by the authors, Mineralogical Society, Monograph 5, London, 1980, p.308.
16. *Mineral Powder Diffraction File-Data Book*, Published by the JCPDS, International Centre for Diffraction Data, USA, 1980.
17. Volzone, C.; Aglietti, E.F.; Scian, A.N.; Porto López, J.M. *Appl. Clay Science* **1987**, *2*, 97.
18. Volzone, C.; Garrido, L.B.; *Appl. Clay Science* **1991**, *6*, 143.
19. Plee, D.; Borg, F.; Gatineau, L.; Fripiat, J.J. *J. Am. Chem. Soc*., **1985**, *107*, 2362.
20. Sanz, J.; Serratosa, J.M. *J. Am. Chem. Soc*. **1984**, *106*, 4790.
21. Sherrif, B.L.; Grundy, H.D. *Nature* **1988**, *332*, 819.
22. Preston, C.M.; Newman, R.H.; Rother, P. *Soil Sci*. **1994**, *157*, 26.
23. Gates, W.P.; Stucki, J.W.; Kirkpatrick, R.J. *PhysChem. Minerals* **1996**, *23*, 535.
24. Mehra, O.P.; Jackson, M.L. *Clays & Clay Min*. **1960**, *7*, 317.
25. Singer, M.J.; Bowen, L.H.; Verosub, K.L.; Fine, P.; TenPas, J. *Clays & Clay Min.* **1995**, *43*, 1.
26. Morris, H.D.; Bank, S.; Ellis, P.D. *J. Phys. Chem*. **1990**, *94*, 3121.